The 2013 World Congress on
Advances in Structural Engineering and Mechanics (ASEM13)
Jeju, Korea, September 8-12, 2013

The Erosion in a Model of Dam-Break Shear Flows

Ya-Ting Huang[1)] and *Yih-Chin Tai[2)]

[1),2)] *Department of Hydraulic and Ocean Engineering, National Cheng-Kung University, Tainan 70101,Taiwan*
[2)] *yctai@mail.ncku.edu.tw*

ABSTRACT

While water surging over a loose sediment bed, the bed material could be taken away with the flows, so that erosion occurs. The sediment material might be captured into the bed in the deposition process. Either in erosion or by deposition, the basal surface evolves due to the mass exchange through the interface between the flowing layer and the stagnant bed. In the present study, a three-layer structure along the flow thickness is considered, where a pure water layer lies above a mixture layer of water and grains, and they flows over a water-saturated granular substratum. Different to the model in (Fraccarollo & Capart 2002), we postulate that the mixture transport layer is sheared and exhibits a discontinuity of sediment concentration at the interface between the mixture layer and the substratum. We incorporate Unified Coordinate method (Tai and Kuo, 2008; Tai et al. 2012) to describe the deforming basal surface, while erosion and/or deposition occurs. The resulting model equations are implemented by a Non-Oscillatory Central (NOC) scheme, in which the meshes move and coincide with the deforming basal surface simultaneously. The numerical examples illustrate the features of the proposed approaches and the theoretical predictions compare favorably with experimental measurements.

1. INTRODUCTION

About 60% area of Taiwan island is covered by mountains and hills. In summer, the typhoon season, there are frequently abundant heavy rainfall events. Due to the towering mountains and steep slopes, the water rushes very fast which results in serious erosion in the upstream section, and the downstream area is suffering from the debris deposition. In recent years, we are encountering heavy rainfall likely caused by the extreme climates, such as the Morakot typhoon in August 2009, which is the most severe flooding after 1950 in Taiwan. in the early morning of August 9, the heavy rainfall triggered a huge landslide, which built a short-lived block dam with life of about 20 minutes in Chishan river (Dong et al., 2011). The dam broke, where the water and the consequent debris flowed downstream and buried a small village, the Xiaolin village. According to the report by the National Disaster Prevention and Protection Commission, R.O.C. (NDPPC), 480 people were buried alive in this catastrophic incident. And according to the statistics of National Fire Agency, death toll was 769 people since Morakot typhoon.

Kuo et al (2011) reconstructed the Xiaolin landslide by a single-phase, shallow-water-like model in a coordinate system of general topography. In the present study, we focus on the flow behavior with erosion and deposition after the dam breaks. A curvilinear coordinate system for general topography is adopted, which coincides with the deformable basal surface.

A simplified two-layer theory has been applied by Fracarollo and Capart (2002), in which it is considered that a pure water layer lies above a water-grain mixture layer, and these two layers flow over a water-saturated granular substratum. In this simplified two-layer theory, a unique and uniform velocity distribution along the flow thickness is assumed for the pure water and the mixture layer, and the mixture layer and the granular substratum are assumed to be of the same sediment concentration. These two assumptions may not meet the reality. In the present work, we proposed a non-uniform velocity distribution for the mixture layer and allow the concentration difference between the mixture layer and the bottom material.

The resultant model equations are implemented for numerical simulation by a shock-capturing, Riemann-solver-free approach, the non-oscillating central (NOC) scheme by Jiang and Tadmor (1998). The code is first validated by the Ritter's dam break solution (Ritter, 1892) over a dry rigid bed, and by the Stoker's solution for a dam-break wave into a region of still tail water. The numerical results reveal the applicability of the proposed theory to capture the deformable basal surface, due to the erosion and deposition of the sediment.

2. Model equations

2.1 Coordinate system

Consider two coordinates systems: the horizontal-vertical Cartesian coordinate system and the terrain-fitted coordinate system see Fig. 1. Let (x,z) be the Cartesian coordinate with x-coordinate laying on the horizontal plane and z-axis pointing the vertical direction against the gravity. On the topographic surface, a terrain-fitted coordinate system (ξ,ζ) is introduced that where ξ -coordinate lays in the basal surface and ζ denotes the normal direction. Let $F_b = z - b(t,x)$ denotes the topographic surface. And the normal vector of the surface $\vec{n}$ can be given by

$$\vec{n} = \frac{\nabla F_b}{|F_b|} = -c\frac{\partial b}{\partial x}\boldsymbol{e}_x + c\,\boldsymbol{e}_z = -s\,\boldsymbol{e}_x + c\,\boldsymbol{e}_z, \tag{1}$$

where $s = \partial_x b\left(1+\left(\partial_x b\right)^2\right)^{-1/2}$ and $c = \left(1+\left(\partial_x b\right)^2\right)^{-1/2}$. Hence, the vector of any point at a distance ζ over the basal surface can be expressed as

$$\vec{r} = r_x\,\boldsymbol{e}_x + r_z\,\boldsymbol{e}_z = \vec{r}_b + \zeta\,\vec{n} = \left(x-\zeta\,s\right)\boldsymbol{e}_x + \left(b+\zeta\,c\right)\boldsymbol{e}_z\,. \tag{2}$$

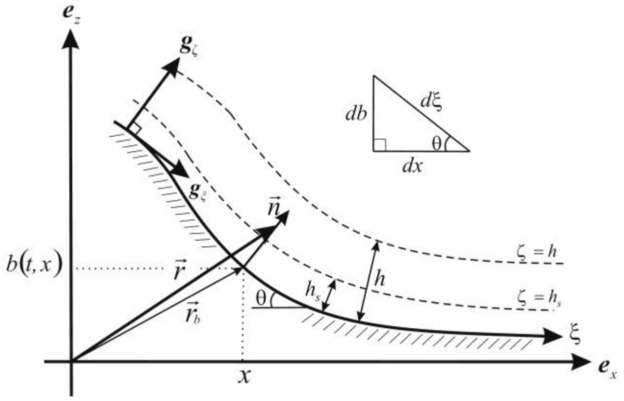

Fig. 1 The Cartesian coordinate system (x, z) and the terrain-fitted coordinate system, where $\vec{n}$ is the unit normal vector.

The topography may vary due to the erosion/deposition. The terrain-fitted coordinate system and Cartesian can be related by the unified coordinate (UC) method,

$$d\vec{r} = \vec{Q}\,dt + \mathbf{\Omega}\,d\vec{\xi} \tag{3}$$

where $\vec{Q}$ is the local coordinate velocity and $\mathbf{\Omega}$ is the Jacobian matrix, see e.g. Hui (2007) or Tai et al. (2012). The component of $\mathbf{\Omega}$ in (3) is given as following

$$\mathbf{\Omega} = \begin{pmatrix} 1 & -s_x \\ s_x/c & c \end{pmatrix} \begin{pmatrix} (1-\zeta\partial_x s)\partial_\xi x & 0 \\ 0 & 1 \end{pmatrix}, \tag{4}$$

and the local coordinate velocity is set to be equal to the velocity of the basal surface, i.e. the erosion/deposition rate. Since there are two coordinate systems, any physical quantities are of two forms, given in either of the systems. For example, the velocity $\vec{u}$ can be expressed by

$$\vec{u} = u^x \boldsymbol{e}_x + u^z\,\boldsymbol{e}_z = u^\xi \boldsymbol{g}_\xi + u^\zeta\,\boldsymbol{g}_\zeta. \tag{5}$$

With the assumption that the flow body is very thin and the slope changes gently, the Jacobian matrix can be approximated by

$$\mathbf{\Omega} \approx \mathbf{\Omega}_b = \begin{pmatrix} 1 & -s_x \\ s_x/c & c \end{pmatrix} \begin{pmatrix} \partial_\xi x & 0 \\ 0 & 1 \end{pmatrix} \tag{6}$$

and the tangential basis vector $\boldsymbol{g}_\xi \approx \boldsymbol{\tau}_\xi$ throughout the flow depth, see e.g. Tai et al. (2012).

2.2 Governing Equations

We consider shallow dam break flows over erodible bottom. The flow structure is shown in Fig. 2, where a clear water layer with uniform velocity profile flows over the mixture layer. The velocity profile of the mixture layer is assumed to be parabolic and its sediment concentration ϕ_s is different to the one of the substratum ϕ_b. And a hydro-static pressure p_m is assumed for the whole flow body.

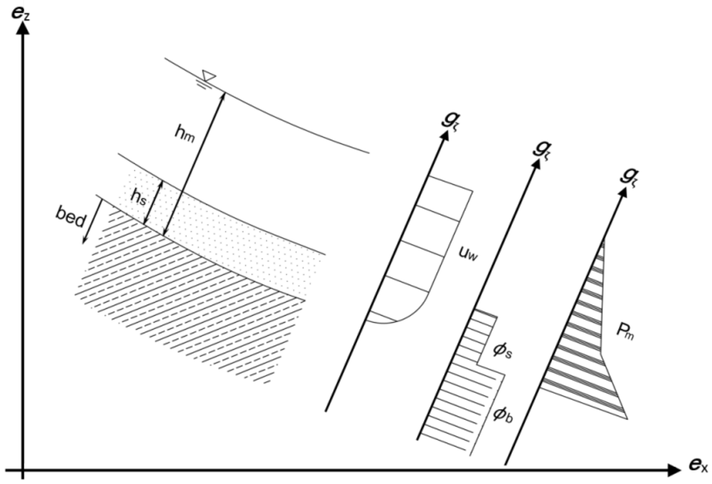

Fig. 2 The flow structure, where p_m is the pressure, ϕ_s is the sediment concentration of the mixture layer and ϕ_b is the concentration of the substratum.

The total flow and mixture layer thicknesses are respectively expressed by h_m and h_s, respectively. Let u^ξ denote the tangential component of the depth-averaged flow velocity and u^x drepresents its x-component. With $J_b = \det(\Omega_b)$, the leading order, depth-integrated equations of mass conservation read

$$\partial_t \left(J_b h_m\right) + \partial_\xi \left(J_b h_m u^\xi\right) = -J_b \frac{\phi_s}{\phi_b} \mathsf{E}, \tag{7}$$

$$\partial_t \left(J_b h_s\right) + \partial_\xi \left(J_b h_s u^\xi\right) = -J_b \mathsf{E}, \tag{8}$$

where (7) is the conservation of the total mass, (8) indicates the conservation of the mixture layer, and **E** represents the deposition rate. The leading order, depth-integrated momentum equation is

$$\begin{aligned} &\partial_t \left(J_b \left(h_m + r h_s\right) u^x\right) + \partial_\xi \left(J_b \left[\beta \left(h_m + r h_s\right) u^x u^\xi + \Sigma^{x\xi}\right]\right) \\ &\qquad = -J_b \left(1 + r\right) u_b^x \mathsf{E} - J_b s_\rho c \left(h_m + r h_s\right) g^x, \end{aligned} \tag{9}$$

where $s_\rho = \rho_s/\rho_w$, $r = (\rho_s/\rho_w - 1)\phi_s = (s_\rho - 1)\phi_s$ and g^x is the x-component of the gravitational acceleration. In (9), $\Sigma^{x\xi} = 0.5c\,g\left(h^2 + rh_s^2\right)\partial_\xi x$ is the depth-integrated stress term and β is the correction factor due to the non-uniform distribution of the velocity. With the assumption of a parabolic profile for the mixture layer, the mean velocity and the mean value of the velocity square over the flow thickness are

$$\bar{u} = \left(1 - \frac{h_s}{3h_m}\right)u_w \quad \text{and} \quad \overline{u^2} = \left(1 - \frac{h_s}{2h_m}\right)u_w^2, \tag{10}$$

respectively, where u_w is the velocity of the clear water layer. By virtue of (10), we deduce the factor β

$$\beta = \frac{\overline{u^2}}{\bar{u}^2} = \left(1 - \frac{h_s}{2h_m}\right)\left(1 - \frac{h_s}{3h_m}\right)^{-2}. \tag{11}$$

2.3 Erosion rate

There is mass flux across the basal surface in erosion/deposition, so that the basal surface is a non-material surface. With the help of the jump conditions of mass and momentum balances (Hutter and Joehnk, 2004), the normal speed of the surface can be determined by

$$\mathrm{E} = \frac{t_G^{\xi\zeta} - t_m^{\xi\zeta}}{\rho_w(1+r)u^\xi} \tag{12}$$

with $t_G^{\xi\zeta}$ the shear stress below the ground surface and $t_m^{\xi\zeta}$ the shear stress above the basal surface. For the shear stress of the mixture layer $t_m^{\xi\zeta}$, a form similar to the Chézy equation in open-channel hydraulics is adopted, (Chow, 1973)

$$t_m^{\xi\zeta} = \rho_s C_f \left|u^\xi\right| u^\xi = s_\rho \rho_w C_f \left|u^\xi\right| u^\xi, \tag{13}$$

in which C_f is an empirical dimensionless coefficient. The bottom shear stress $t_G^{\xi\zeta}$ is assumed to follow the Coulomb's friction law (Lambe and Whitman, 1969) without viscous effect,

$$t_G^{\xi\zeta} = \tan\phi\,\sigma_{bn}' \frac{u^\xi}{\left|u^\xi\right|}, \tag{14}$$

where ϕ is the angle of the internal friction of the sediment, and σ_{bn}' is the effective normal stress. With Terzaghi's principle (Lambe and Whitman, 1969) and the hydrostatic assumption, the effective normal stress in (14) is given by

$$\sigma_{bn}^{'} = t_G^{\zeta\zeta} - p_w = \rho_w g\, r\, h_s c, \tag{15}$$

Note that the effective normal stress $\sigma_{bn}^{'}$ is function of the concentration ϕ_s and which is of different value at bottom ϕ_b .

3. Numerical Study

3.1 Dam break flows over rigid bed

In this section two benchmark problems are simulated by the implemented simulation code. The first example is the exact solution of the dam break flow by Ritter (1892), in which a uniform water body is suddenly released and flows over a dry horizontal plane. The second numerical example is the simulation of the Stoker's solution (Stoker, 1957), where the uniform water body is released and merges into a thin still water layer. Figure 3 illustrates the sequential results of Ritter's solution and Fig. 4 exhibits the simulated results of Stoker's solution. Here and hereafter in the figures, the blue solid lines indicate the exact solutions, the red dashed lines are the numerical results, and the blue thick solid lines represent the horizontal basal surface. The numerical results show excellent agreements in both of the above exact solutions. In these two numerical examples, neither erosion nor deposit is taken into account. The agreements between simulation and analytical solutions reveal the applicability of the UC approach for the flows over rigid bed.

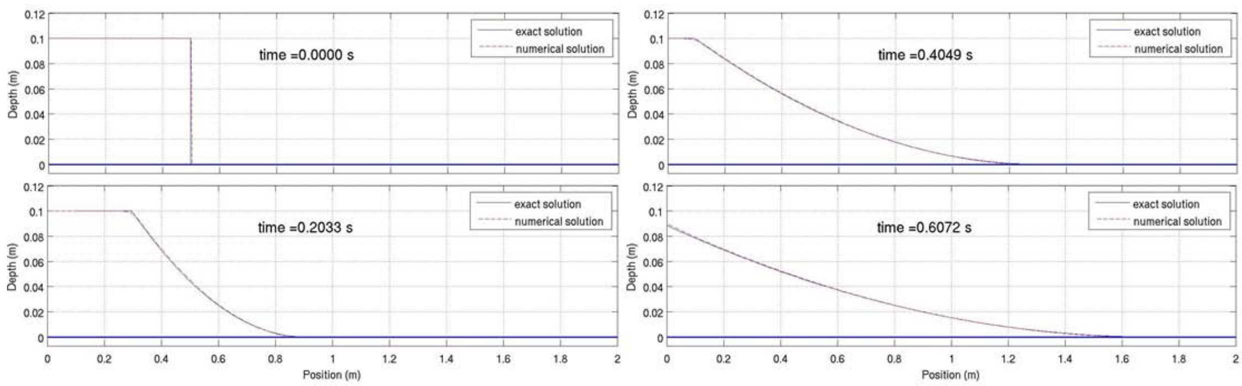

Fig. 3 Numerical results for Ritter's exact solution

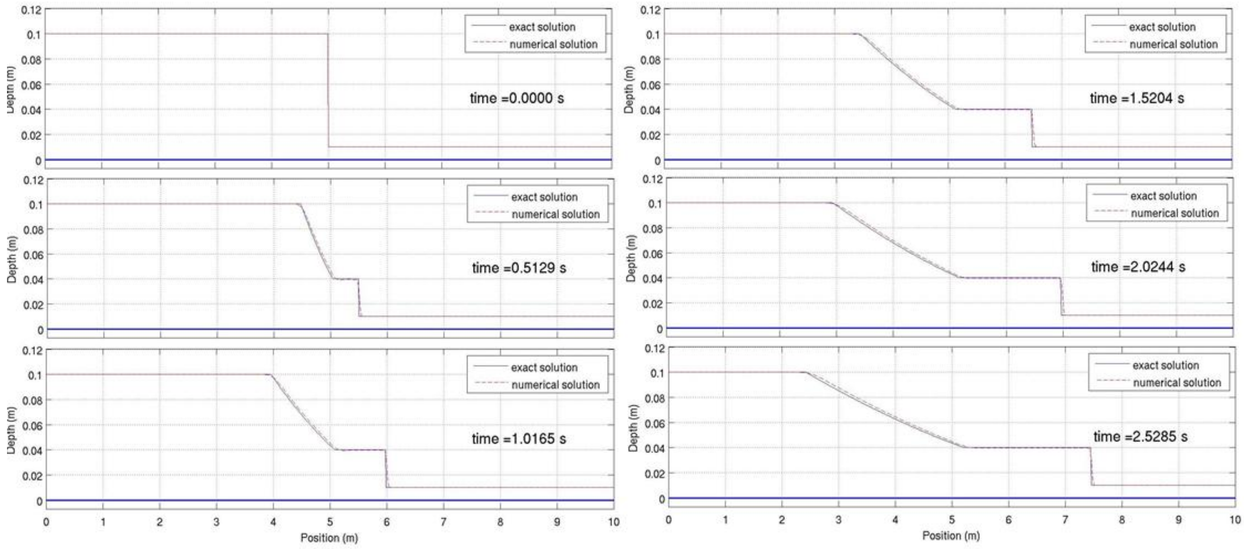

Fig. 4 The simulation of Stoker's solution.

3.2 Dam break flows over erodible bed

In this section, numerical simulation with erosion/deposition is considered. The results shown in Figs. 5 and 6 are computed with uniform velocity distribution both in the clear water and mixture layers. The left panel of Fig. 5 shows the results computed with $\phi_s = \phi_b$ =0.5. In the right panel is the results with ϕ_s =0.4096 and ϕ_b =0.512, which is the values of the bottom sediment concentration suggested by Egashira (1999). With $\phi_s = \phi_b$ =0.5, the flow induces deeper erosion and the front travels significantly faster. The phenomena might be due to the bottom sediment concentration and the proposal of the erosion rate (12). With fixed bottom sediment concentration ϕ_b =0.512, we consider the effect of the concentration of the mixture. Figure 6 shows the results computed with ϕ_s = 0.4096 (left panel) and 0.4608 (right panel), respectively. The results in Fig. 6 reveals that small value of ϕ_s induces faster transportation.

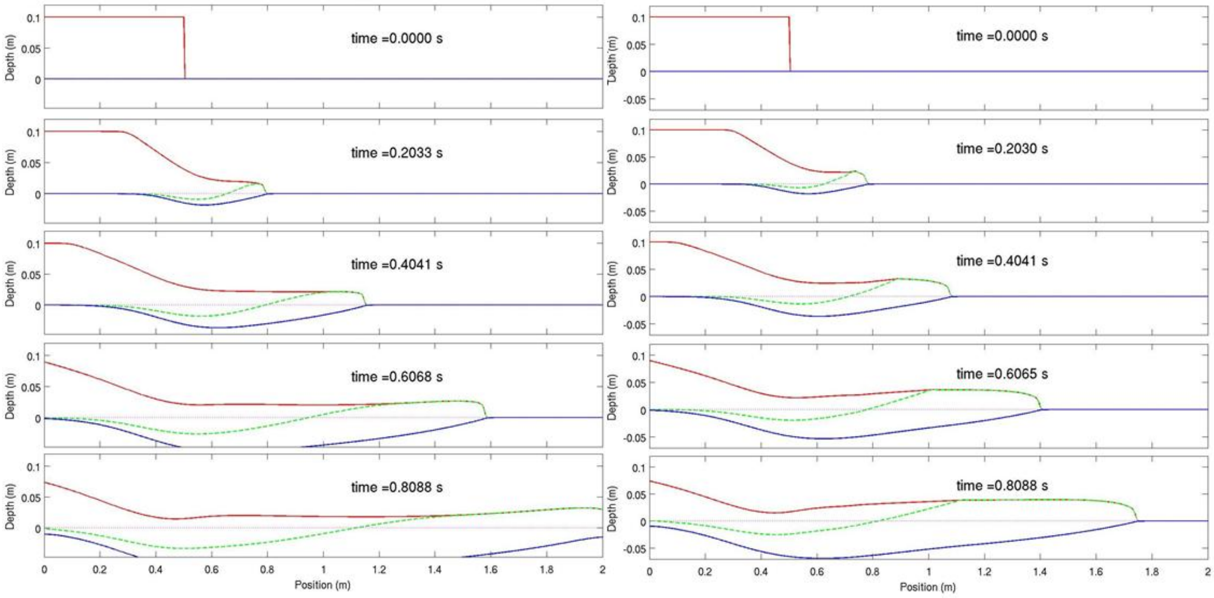

Fig. 5 Left: ϕ_s=0.5, ϕ_b =0.5; Right: ϕ_s=0.4096, ϕ_b =0.512

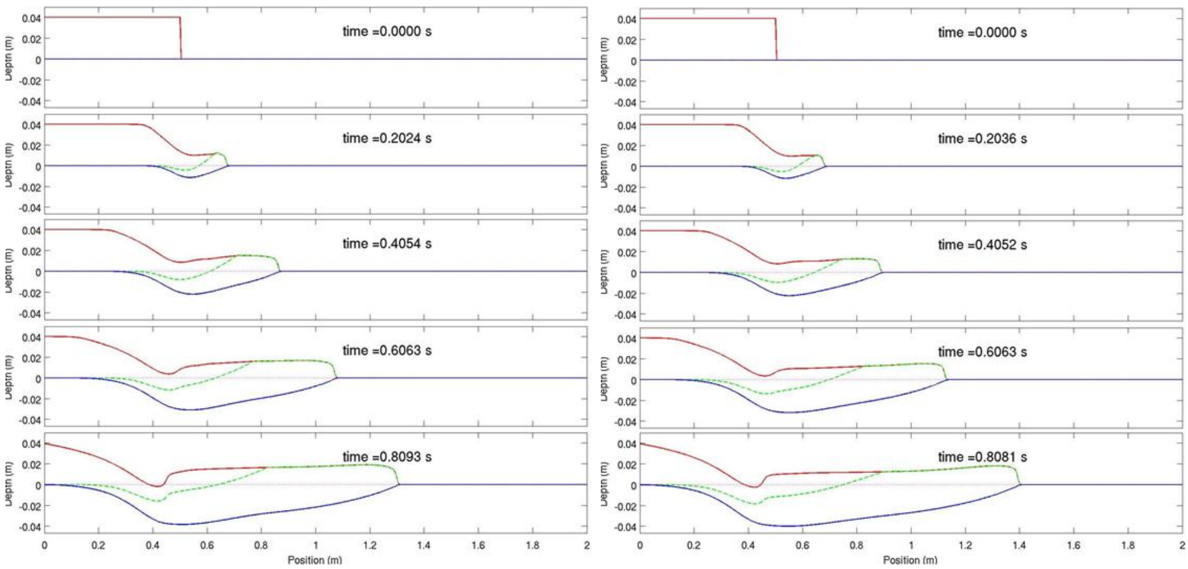

Fig. 6 Left: ϕ_s=0.4096, ϕ_b=0.512; Right: ϕ_s=0.4608, ϕ_b =0.512

To study the effect of the velocity distribution in the mixture layer, we consider the condition with ϕ_s = 0.4096 and ϕ_b = 0.512, and the results are shown in Fig. 7. The left panel illustrates the results computed with uniform velocity distribution, and the right panel depicts simulations with non-uniform velocity profile in the mixture layer. It is found that the non-uniform velocity distribution allows a faster movement together with a larger amount of eroded material.

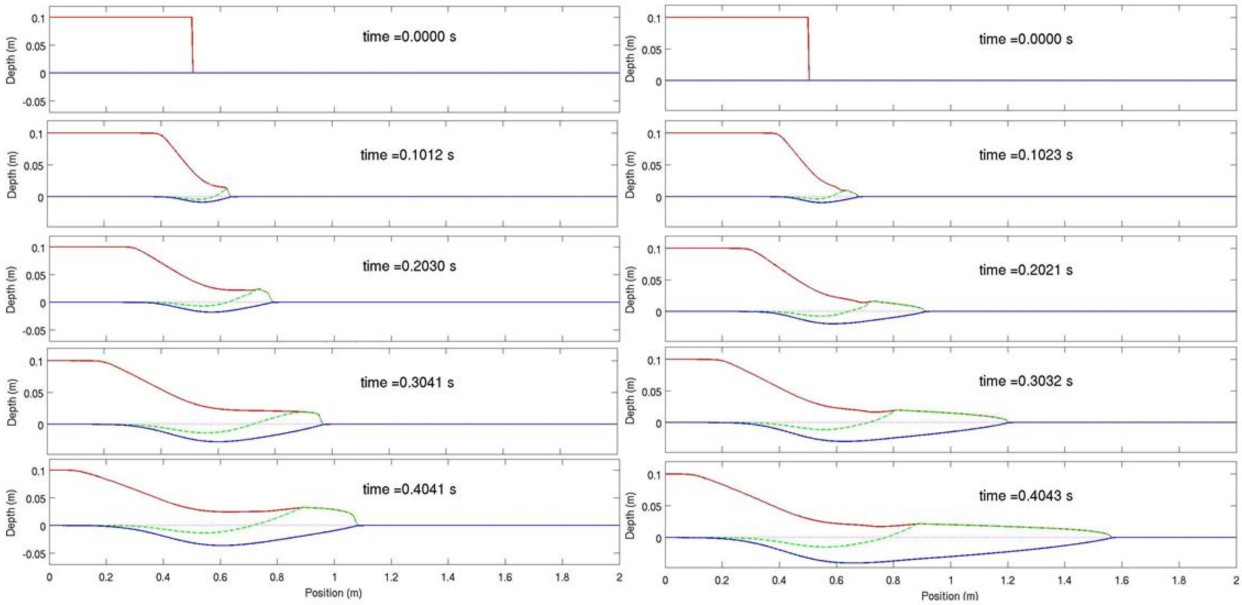

Fig. 7 Left: computation with uniform velocity distribution;
Right: computation with non-uniform velocity distribution.

Figure 8 is the comparison between the experiment (Fraccarollo and Capart, 2002) and the numerical result with respect to the proposed theory. Good agreement is observed between the experimental measurement and simulation. Although favorable comparison has been obtained with the condition of $\phi_s = \phi_b$ =0.5 and with uniform velocity distribution at the first stage, the front travels faster than the numerical results when t $\geq$ 0.6 s (Spinewine and Capart, 2013). The results in Fig. 8 reveal that the proposed theory might improve the drawbacks in the previous model by Fraccarollo and Capart (2002).

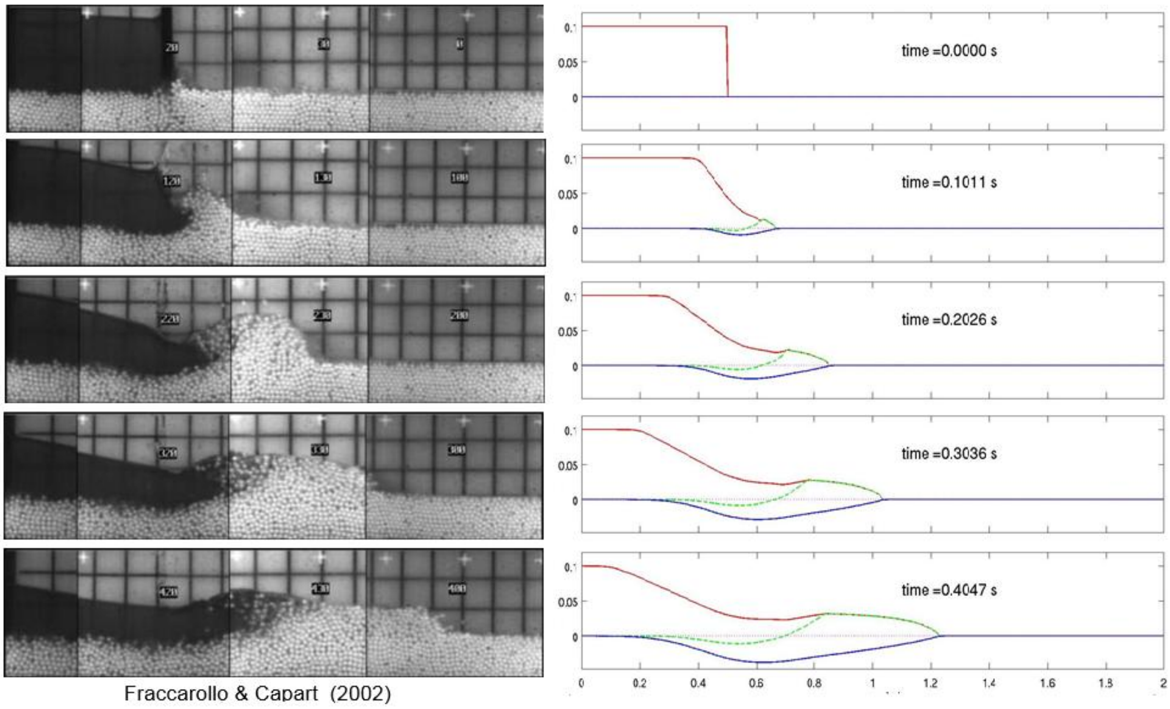

Fig. 8 The experimental observation and the numerical results computed with ϕ_s = 0.3584 and ϕ_b =0.512, where the velocity distribution of the mixture layer is non-uniform.

4. CONCLUSIONS

Based on the simplified model by Fraccarollo and Capart (2002), we introduced a coordinate system for general topography to the model equations, in which the coordinate axis simultaneously coincides with the deformable basal surface. Besides the coordinate system, we postulate a shear layer for the mixture transport layer and a discontinuity of sediment concentration at the interface between the mixture layer and the bottom substratum. Numerical examples are applied for investigating the effect of different values of sediment concentration and the introduction of the shear layer. The comparison with the experimental observation supports the applicability of the proposed theory. The results reveal the wide range of potential applications in hydraulic engineering.

ACKNOWLEDGEMENT: The authors are grateful to the financial support by the National Science Council, Taiwan (Project No.: NSC 101-2628-E-006- 019-MY2).

REFERENCES

Chow, V. T. (1973), *Open-channel Hydraulics.* McGraw-Hill Book Company.

Dong, J.J., Li, Y.S., Kuo, C.Y., Sung, R.T., Li, M.H., Lee, C.T., Chen, C.C. and Lee, W.R. (2011) "The formation and breach of a short-lived landslide dam at Hsiaolin Village, Taiwan—Part I: Post-event reconstruction of dam geometry." *Eng. Geol.*, Vol. **123**, 40-59.

Fraccarollo, L. and Capart, H. (2002), —Riemann wave description of erosional dam-break flows."*J. Fluid Mech*. Vol. **461**, 183-228.

Hui, W.H. (2007). —The Unified Coordinate System in Computational Fluid Dynamics.", *Commun. Comput. Phys.*, Vol. **2**, 577-610.

Hutter, K. and Joehnk, K. (2004), *Continuum Methods of Physical Modeling.* Springer Verlag.

Jiang, G.S. and Tadmor, E. (1998), —Non-oscillatory central schemes for multidimensional hyperbolic conservation laws." *SIAM. J. Sci. Comp.*, Vol. **19**, 1892–1917.

Kuo, C.Y., Tai, Y.C., Chen, C.C., Chang, K.J., Siau, A.Y., Dong, J.J., Han, R.H., Shimamoto, T., and Lee, C.T. (2011), —The landslide stage of the Hsiaolin catastrophe: Simulation and validation.", *J. Geophys. Res.*, Vol.**116**, F04007, doi:10.1029/2010JF001921

Lambe, T. W. and Whitman, R. V. (1969), *Soil Mechanics.* John Wiley, New York.

Ritter, A. (1892), "Die Fortpflanzung der Wasserwellen." *Zeitschrift Verein Deutscher Ingenieur*, Vol. **36**, 947-954.

Spinewine, B. and Capart, H. (2013),"Intense bed-load due to a sudden dam-break." *J. Fluid Mech.* (in press).

Stoker, J. J. (1957), *Water Waves: The Mathematical Theory with Applications.* Whiley-Interscience.

Tai, Y.C. and Kuo, C.Y. (2008), —A New Model of Granular Flows over General Topography with Erosion and Deposition." , *Acta Mechanica*, Vol. **199**, 71-96.

Tai, Y.C. and Kuo, C.Y. (2012), "Modelling shallow debris flows of the Coulomb-mixture type over temporally varying topography." *Nat. Hazards Earth Syst. Sci*., Vol. **12**, 269– 280.

Tai, Y.C., Kuo, C.Y. and Hui, W.H. (2012), —An alternative depth-integrated formulation for granular avalanches over temporally varying topography with small curvature." *Geophysical & Astrophysical Fluid Dynamics*, Vol. **106**, 596-629.